Journal of Sound and Vibration (2002) **257**(4), 753–777
doi:10.1006/jsvi.5093, available online at http://www.idealibrary.com on IDEAL®

VALIDITY AND APPLICABILITY OF TWO SIMPLE HYSTERESIS MODELS TO ASSESS PROGRESSIVE SEISMIC DAMAGE IN R/C ASYMMETRIC BUILDINGS

S. C. Dutta and P. K. Das

Department of Applied Mechanics, Bengal Engineering College, Howrah 711103, *India.*
E-mail: prithwishbec@netscape.net

(*Received* 30 *July* 2001, *and in final form* 6 *December* 2001)

The coupled lateral–torsional vibration in R/C asymmetric structures under seismic loading leads to larger lateral deformation in the load-resisting elements located at one edge, compared to the other resisting elements. This may cause earlier yielding of the elements of that edge in localized form. Strength and stiffness degradation due to successive inelastic excursions of these R/C structural elements at one edge may make these elements more flexible and weaker as compared to those at the opposite edge. This may cause progressive shifting of stiffness and strength centres away from this flexible edge, leading to consequent increase of effective eccentricity in successive loading cycles. This, in turn, causes a progressive increase in torsional effect in R/C structures. This damaging effect cannot be predicted by using the bilinear hysteresis models devoid of degradation characteristics. Existing sophisticated hysteresis models representing the degrading behaviour of the R/C structural load-resisting elements require a number of parameters to be specified, the evaluation of which requires extremely case-specific calibration study. In this context, the present paper studies the suitability of two alternative simplified hysteresis models, which are capable of predicting the strength and stiffness degrading behaviours with simple input parameters. Responses of idealized asymmetric R/C building systems are studied using these two hysteresis models under design spectrum-consistent synthetic ground motions and idealized near-fault ground motions. The comparison between the responses of the R/C asymmetric structures with deteriorating structural elements and the similar structures having elasto-plastic structural elements proves the suitability of the proposed models in recognizing the progressive damaging effect of torsion in R/C asymmetric buildings.

1. INTRODUCTION

Due to an initial eccentricity between the centre of mass (CM) and the centre of stiffness (CS), lateral–torsional coupled vibration causes yielding of structural elements at one edge earlier than the opposite edge, when an asymmetric structural system is subjected to seismic excitation. Hence, R/C structural elements of this edge undergo considerably larger degradation in strength and stiffness as compared to elements on the opposite sides, due to such yield excursions under successive cycles of loading. This causes continuous shifting of the centre of resistance (CS) away from the edge with deteriorated structural elements and from the centre of mass. As a result, the torsional effect increases due to increase in the effective eccentricity. This further aggravates the torsional damage by increasing the numbers and extent of yield excursions and thereby causing further deterioration in strength and stiffness of the same edge elements. This may lead to failure of asymmetric buildings because of excess ductility demand generated locally at structural elements of one

0022-460X/02/$35.00

edge. Such failures were observed in many past earthquakes, e.g., 1985 Mexico earthquake and the 1995 Kobe earthquake in Japan. One R/C building with mass eccentricity severely damaged in the recent Gujarat earthquake of 26 January 2001, in India, well demonstrates this typical problem [1].

R/C structural elements undergo progressive stiffness and strength deterioration with increasing number of yield excursions due to repetitive load [2]. On the other hand, most of the existing studies on the inelastic behaviour of asymmetric buildings have generally adopted a bilinear elasto-plastic hysteresis behaviour for the structural load-resisting elements. Hence, these studies cannot recognize the progressive effect of damage due to torsion likely to be concentrated at one edge of the asymmetric R/C structures as apprehended in the literature [2]. A recent study [3] on the behaviour of asymmetric buildings shows that even the incorporation of only strength deterioration in hysteresis behaviour may increase the response considerably. However, a realistic estimate of the seismic response of R/C asymmetric buildings can be made only if both the strength and stiffness degradation are incorporated in the hysteretic behaviour of structural elements. A number of sophisticated hysteresis models are available in the literature, e.g., three-parameter model [4], Roufaiel–Meyer model [5], etc. A comprehensive list of such models is available elsewhere [6]. Use of these sophisticated models requires extremely case-specific calibration of the parameters involved. Such calibration is dependent on the rigorous details of the structural members, e.g., dimensions, grade of concrete, details of longitudinal as well as transverse reinforcements, etc. On the contrary, studies on the inelastic seismic torsional behaviour of asymmetric buildings (e.g., the studies listed in the literature [2]) model structural elements (frame or walls) in the overall sense by representing them through lateral load-resisting elements with adequate stiffness, strength and simple hysteresis rules.

A simple hysteresis model, which was proposed and used in one of the recent studies [7] on seismic behaviour of R/C asymmetric buildings, can account for both stiffness and strength degradation. Stiffness degradation in this model is accounted through degrading the inclination of the loading branch by a certain fraction α. The fraction α is the average angular drop in inclination due to each inelastic excursion. Thus, the value of α is dependent on the units of force and displacement chosen for experimental studies. Hence, the result may vary depending on units chosen.

In this context, the present paper proposes two simple hysteresis models, which can account for stiffness and strength deterioration characteristics of R/C structural elements under cyclic loading. These models overcome the bottleneck of the model discussed above. A preliminary study considering these two hysteresis models was reported in a conference [8] in a very limited form. The present paper is an effort to make a comprehensive study of all the significant aspects of the performance of these models to arrive at conclusive ends. The performances of the hysteresis models are studied through the comparison of a number of load–deformation curves produced by the models with those obtained experimentally under similar cyclic displacement histories, collected from a number of recent studies available in the literature [9–16]. The comparison of the total hysteretic energy dissipation through experimental and computed load–deformation curves is also presented for each of the repetitive displacement histories. The performances of the stiffness-degrading model, strength-deteriorating model and frequently used bilinear elasto-plastic model are also presented to show the relative advantages of the proposed models. The proposed models, especially the first one, are concluded to be suitable due to firstly, the reasonable accuracy in reproducing experimental load–displacement history as well as total hysteretic energy dissipated during the history of shaking and secondly the convenience of calculation of the degradation parameters involved. It is also attempted to see how small the time step of

numerical integration will be, in comparison to the natural period of the systems, to achieve sufficient accuracy in response for the bilinear model and two proposed models. Such a comparison helps to evaluate the level of computational effort required if these models are used. The performances of the proposed models to recognize progressive torsional damage due to asymmetric yielding of lateral load-resisting elements are also demonstrated through limited case studies of asymmetric building systems under seismic excitation.

2. DETAILS OF TWO HYSTERESIS MODELS

The stiffness degradation and strength-deterioration characteristics are incorporated with a bilinear backbone curve in both the models to represent the hysteresis behaviour of structural load-resisting elements. Different researchers have used various post-yield stiffness, ranging from fully plastic to 5% strain-hardening ratio [2]. Though it may be a source of variance in the results, the variation does not appear to be significant [2]. Hence, in the absence of any well-accepted value for the strain-hardening ratio, the bilinear backbone curve is chosen as elastic–perfectly plastic.

In both the models, the yield strength is deteriorated by a fixed fraction δ of the original yield strength F_y due to each yielding to model the strength deterioration. The stiffness of the elastic loading portion of the load–displacement curve in the first model is obtained using the principle similar to that of Takeda's model [17]. The elastic loading branch targets the previous point of unloading on the same side (either positive or negative) of the load history, and thus the new deteriorated loading stiffness is calculated. In case of the second model, the loading stiffness is degraded by a fixed fraction α of the initial loading stiffness k after each yielding. Unloading elastic stiffness remains the same as initial stiffness before and after yielding for both the models. The first model involves only three input parameters, namely initial yield strength F_y, initial loading stiffness k and rate of strength deterioration δ. The second model requires an additional input parameter, namely rate of the stiffness degradation α, besides the other three parameters of the first model. These modelling schemes can be well understood by two schematic example load–displacement curves obtained from the first and second model, respectively, and presented in Figure 1.

α and δ can be obtained by dividing the total drop in stiffness and strength, respectively, by the number of yield excursions in the experimental load–displacement history of the structural members whose behaviours are to be modelled. Many such experimental curves are available in the literature [9–16]. For modelling the behaviour of any particular structural member, the experimental load–displacement histories for members with similar reinforcement characteristics should be used to find α and δ.

3. PERFORMANCE OF HYSTERESIS MODELS

A number of experimental load–displacement curves are chosen from the literature [9–16] to study the performance of the proposed hysteresis models. For each of the various experimental curves available in the literature, the input parameters F_y and k are directly obtained while α and δ are calculated by dividing the total drop in stiffness and strength, respectively, by the number of yield excursions in the experimental load–displacement history. The displacement history is also tabulated for each of the experimental curves. Using displacement history, F_y, k, α and δ as input, each curve is computationally reproduced using two proposed models separately. The computationally reproduced curves are compared with experimental ones regarding various aspects as described below.

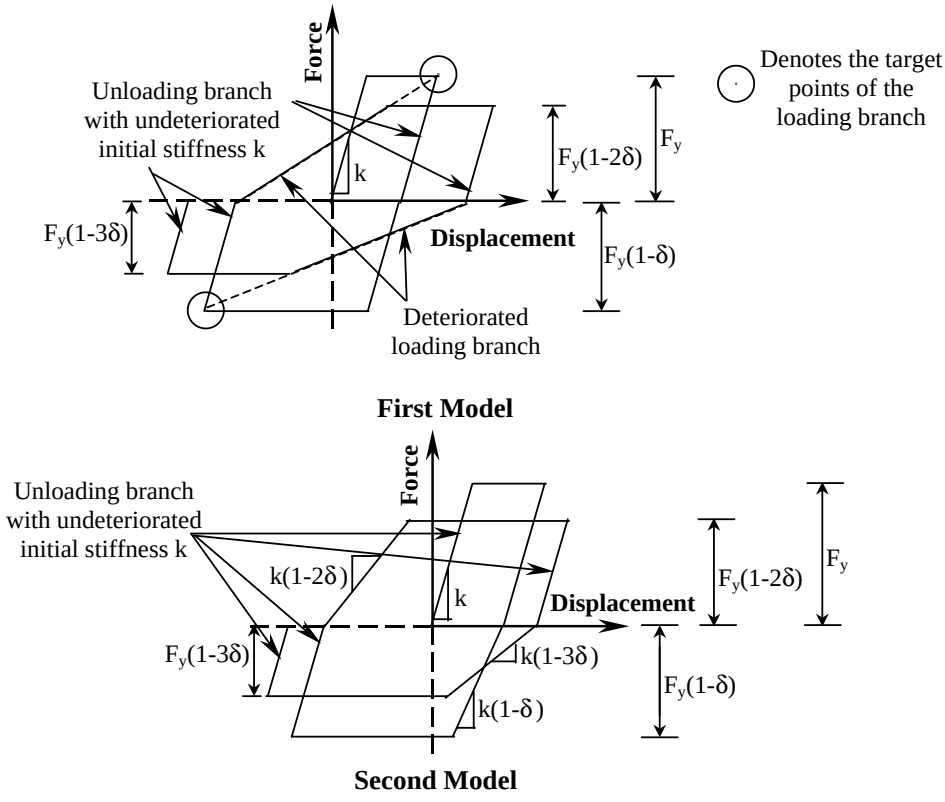

Figure 1. Example load–displacement curves explaining the schemes of the two proposed models.

3.1. PREDICTION OF EXPERIMENTAL CURVES

The reproduced load–displacement curves are compared to corresponding experimental curves to study their closeness with experimental ones. Figures 2–5 present five different experimental curves and the corresponding computationally produced curves by the two proposed models. The computationally reproduced load–displacement curves using first and second hysteresis models are shown by firm lines, separately, in each figure. Original experimental curves drawn by dotted lines are superposed on each of the computationally reproduced curves for facilitating comparison. The figures reveal that the first model reproduces the experimental curves very closely. The performance of the second model is relatively inferior to the first model.

3.2. HYSTERETIC ENERGY DISSIPATION

The closeness of the total hysteretic energy dissipated through the whole displacement history by the computational models to the energy actually dissipated in the corresponding experiment is another important measure of the accuracy of the computational models. Table 1 presents a comparison of the hysteretic energy dissipation through the experimental behaviour and that through the computational models. The energy dissipation by a purely elasto-plastic model, by a model incorporating only stiffness degradation using the same principle as used in the first model, and that incorporating only strength deterioration is also presented in the same table for the sake of comparison. Errors in each case with respect

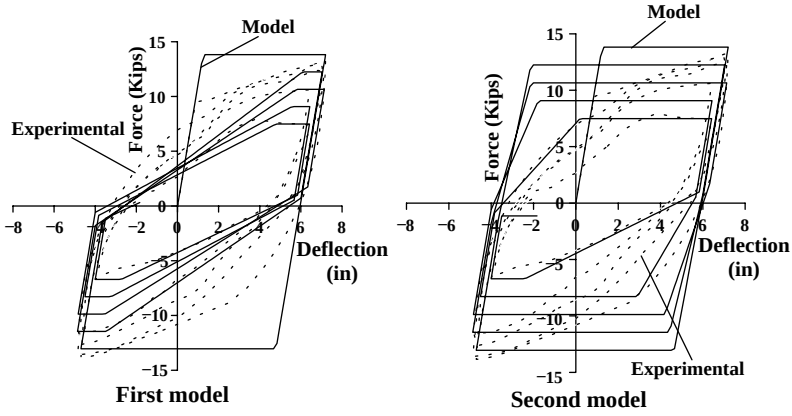

Figure 2. Computationally reproduced hysteresis curves by proposed models from the experimental curve for specimen 88-35-RV10-60, presented by Brown and Jirsa [9].

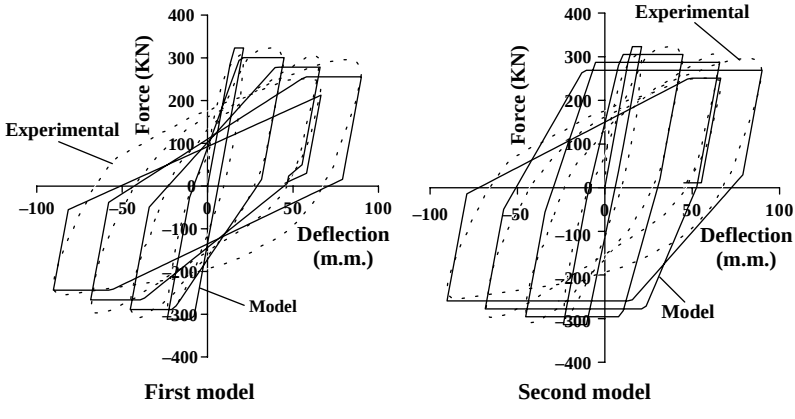

Figure 3. Computationally reproduced hysteresis curves by proposed models from the experimental curve for specimen U6, presented by Saatcioglu and Ozcebe [10].

to the corresponding experimental energy dissipation are also presented. Table 1 reveals that the elasto-plastic model produces considerably large error. This error may be as high as 260%. The lack of accuracy in only stiffness-degrading and only strength-deteriorating models is lesser than the merely elasto-plastic model but the error is still substantial. The maximum error exhibited in energy dissipation by only stiffness-degrading model is 58% and that by only strength-deteriorating model is 137%, as shown in Table 1. The error exhibited by the proposed first model is always less than 15%, while the maximum error exhibited by the second model is 103% in one case, but in other cases the performance is superior to elasto-plastic, only stiffness-degrading and only strength-deteriorating models. The error reduces considerably if both stiffness degradation and strength deterioration are included. Especially, the first model exhibits a very small deviation from experimental results. It is interesting to note that the value of dissipated energy in case of the first model is either less than that of the experimental values or exceeds it by less than only 5% (in a single case). The displacement predicted by a model which dissipates lesser energy than actual will make a higher prediction of displacement demand and, hence, appears to be safe for design purposes.

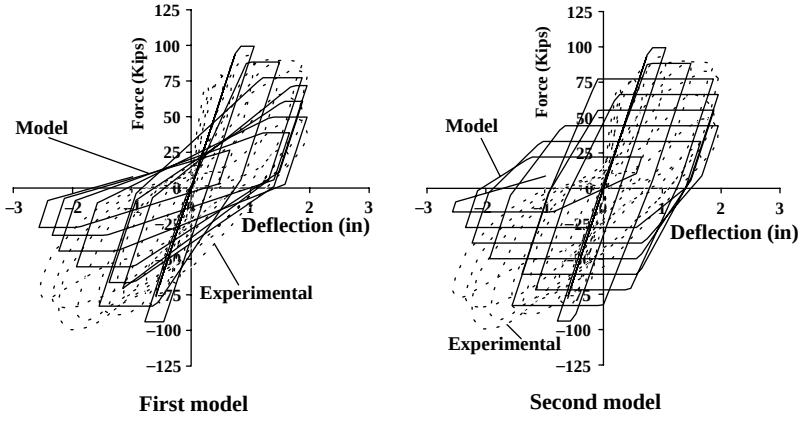

Figure 4. Computationally reproduced hysteresis curves by proposed models from the experimental curve for column 1, presented by Priestley and Benzoni [13].

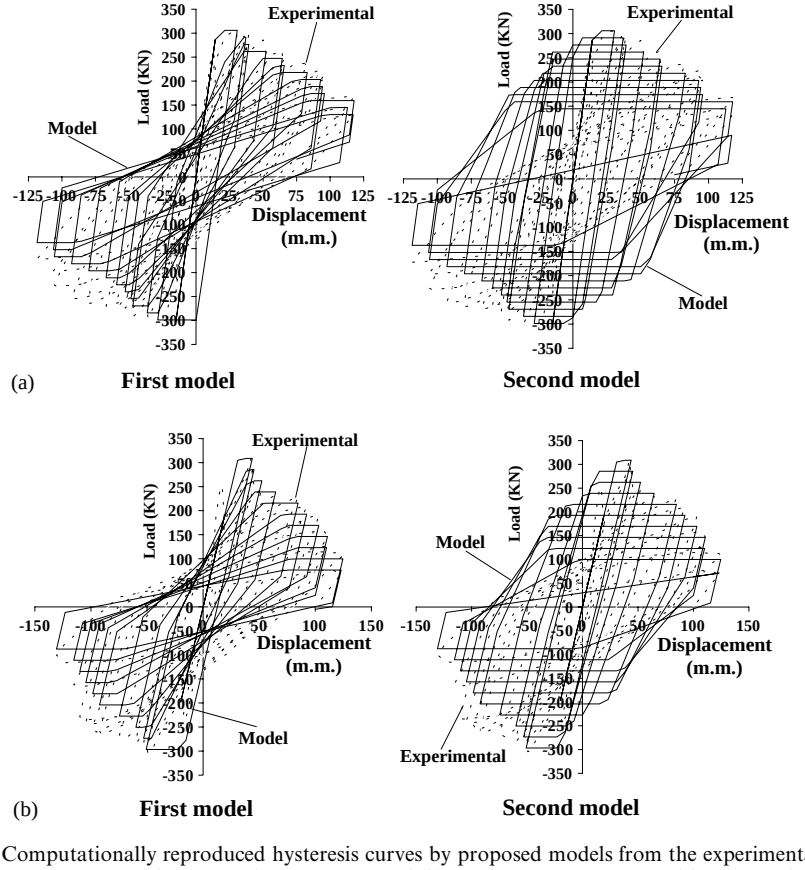

Figure 5. Computationally reproduced hysteresis curves by proposed models from the experimental curve for (a) specimen C1-3, presented by Mo and Wang [16], and (b) specimen C2-3, presented by Mo and Wang [16].

TABLE 1

Energy dissipated in different types of hysteresis models

Source of experimental curves (with unit of energy)	Model type	Energy value	% Deviation from experimental values
Brown and Jirsa [9]	Experimental	632·855	—
Specimen—88-35-RV10-60 (kip in)	Elasto-plastic	1203·123	90·11
	Stiffness degrading	1002·081	58·34
	Strength deteriorating	945·004	49·32
	First model	581·346	− 8·14
	Second model	860·730	36·01
Saatcioglu and Ozcebe [10]	Experimental	131095·00	—
Specimen—U6 (kN mm)	Elasto-plastic	230183·90	75·59
	Stiffness degrading	177223·10	35·19
	Strength deteriorating	202184·30	54·23
	First model	112315·90	− 14·32
	Second model	166779·60	27·22
Priestley and Benzomi [13]	Experimental	1264·858	—
Column 1 (kip in)	Elasto-plastic	2629·655	107·90
	Stiffness degrading	1378·281	8·97
	Strength deteriorating	1729·534	36·75
	First model	1084·109	− 14·29
	Second model	1565·477	23·77
Mo and Wang [16]	Experimental	241789·281	—
Specimen—C1-3 (kN mm)	Elasto-plastic	869681·425	259·68
	Stiffness degrading	365579·596	51·20
	Strength deteriorating	580207·942	139·96
	First model	251911·083	4·19
	Second model	491324·868	103·20
Mo and Wang [16]	Experimental	248824·908	—
Specimen—C2-3 (kN mm)	Elasto-plastic	705580·555	183·56
	Stiffness degrading	360869·337	45·03
	Strength deteriorating	426812·859	71·53
	First model	219241·652	− 11·89
	Second model	361064·569	45·11

4. RECOGNITION OF PROGRESSIVELY INCREASING TORSIONAL EFFECT THROUGH PROPOSED MODELS

4.1. IDEALIZED ONE-STOREY SYSTEM

Seismic torsional response of idealized R/C building systems under simulated ground motion is studied using proposed hysteresis models to examine their suitability in recognizing seismic torsional progressive damage of R/C asymmetric building systems. An idealized one-storey building model as shown in Figure 6 is chosen for studying the difference in inelastic response between symmetric and asymmetric buildings. The same system was also used in earlier studies [7, 8, 18]. This system consisted of a rigid deck supported by three lateral load-resisting structural elements in each of the two orthogonal directions. Hence, this system is referred to as a six-element system for convenience of understanding in the earlier studies [7, 8, 18] as well as in the present study. The lateral

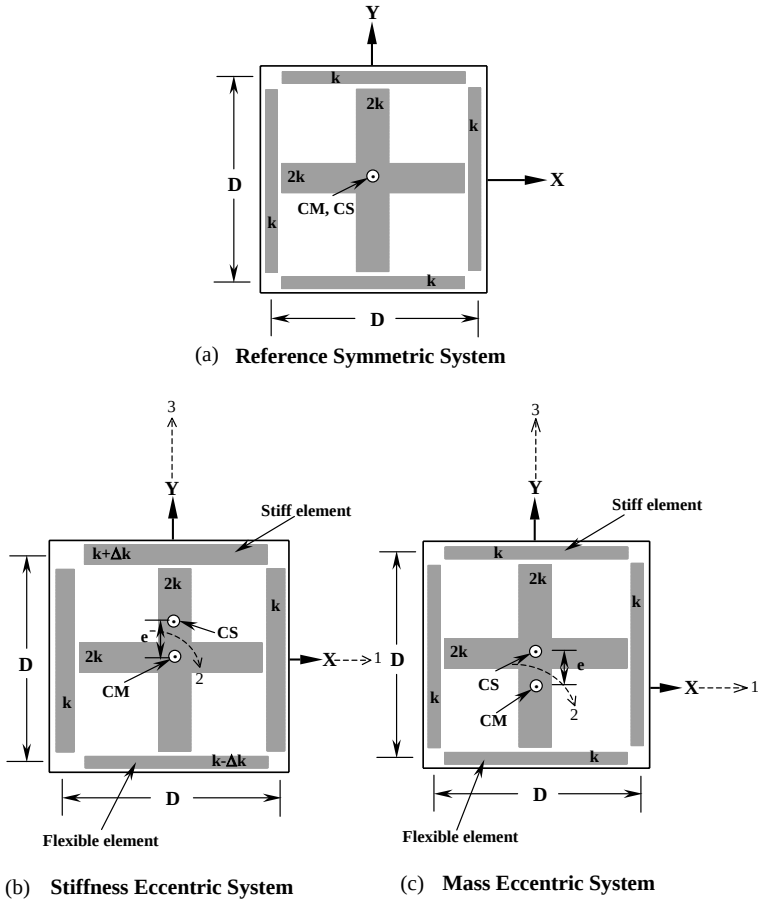

Figure 6. Idealized one-storey building models.

load-resisting structural elements represent frames or walls having strength and stiffness in their planes only. Regular building structures generally have their load-resisting elements uniformly distributed over the plan. Such a distribution in both the orthogonal directions is properly represented in the reference symmetric system (shown in Figure 6(a)), by attributing stiffness $= 2k$ to the middle element which is 50% of the total stiffness $4k$. The remaining 50% is equally distributed among two edge elements such that each of them has stiffness k. The corresponding asymmetric system has the same uncoupled lateral period, T_x, as that of the symmetric system. The required eccentricity e is introduced in the asymmetric system by increasing the stiffness of one edge element and decreasing that of the element at the opposite edge by a calculated amount Δk in case of stiffness-eccentric systems (as shown in Figure 6(b)). For mass-eccentric systems, the stiffness distribution and the location of the centre of stiffness (CS) are initially the same as that of the reference-symmetric system. On the other hand, the centre of mass (CM) is assumed to lie at a distance equal to eccentricity, from the centre of stiffness (CS) (as shown in Figure 6(c)). The edge having a relatively flexible load-resisting element in case of stiffness-eccentric systems and the edge nearer to CM in case of mass-eccentric systems will be displaced more than CM under a lateral load statically applied at CM. This edge is designated as flexible

side and the corresponding edge element as flexible side element or simply flexible element. On the other hand, the opposite edge, having a relatively stiff load-resisting element in case of stiffness-eccentric systems and away from CM in case of mass-eccentric systems, will be displaced less than CM under a lateral load statically applied at CM. This edge is designated as stiff side and the corresponding edge element as stiff side element or simply stiff element. The distances D between two extreme lateral load-resisting elements in two orthogonal directions are the same. Locations of the outermost edge elements are not fixed. Depending on various characterizing parameters of the system, these positions vary in building plan. Several previous studies [19, 20] assumed the outer elements to be located exactly at the edges of the system plan. However, fixing these locations implies additional restrictions and causes lack in generality [21].

4.2. SYSTEM PARAMETERS

The change in maximum displacement demand and hysteretic energy demand may be influenced by several characteristics of the systems as well as loading. Hence, reasonable variations of the influential parameters need to be considered to arrive at meaningful conclusions. Variations of the parameters considered are discussed below very briefly.

4.2.1. *Dynamic characteristics of the system*

The maximum displacement demand and hysteretic energy demand for extreme-edge load-resisting element were studied for a feasible range of dynamic characteristics of the system, i.e., uncoupled lateral period T_x and uncoupled torsional to lateral period ratio τ. Three representative uncoupled lateral periods T_x, namely 0·5 s, 1 s and 2 s, were chosen to represent the typical building systems in short, medium and long period ranges respectively. The values of uncoupled torsional-to-lateral period ratio τ for most of the real buildings are generally within a range of 0·25–2·0. Hence, τ was varied over a range of 0·25–2·0 with an interval of 0·05.

The effect of the mass distribution over the plan area of the rigid deck is reflected through the radius of gyration r of the mass of the same. In fact, the uncoupled torsional to lateral period ratio τ for chosen stiffness distribution of the structural system (as shown in Figure 6) was varied over a range of 0·25–2·0 by varying r as required. Thus, the variation of τ implicitly accounts for the variation in mass distribution.

4.2.2. *Magnitude and nature of eccentricities*

The magnitude and nature of eccentricities influence the torsional response of asymmetric systems. Hence, asymmetric systems with three typical values of eccentricities $e = 0{\cdot}05D$, $0{\cdot}1D$ and $0{\cdot}2D$ were considered as representative of the small, medium and large eccentricity systems. Asymmetric systems with both mass and stiffness eccentricities are considered in the present study.

4.2.3. *Ductility-reduction factor* (R_μ)

A factor called ductility-reduction factor, R_μ, is defined as the ratio of the elastic force demand of a structure to its actual lateral strength provided. The extent of inelastic behaviour exhibited by a structure under a specified loading depends on this ratio. Buildings due to their large redundancies may have R_μ as high as 8 (NEHRP Provisions) [22]. However, they may be designed with $R_\mu = 1$, 2 or 4 depending on their importance

level. Extensive case studies are made with various combinations of T_x, τ, e and R_μ. However, only a few selective case studies are presented involving each of the above-mentioned four values of R_μ for the sake of brevity.

4.3. GROUND MOTIONS

Two artificially generated earthquake time histories consistent with the design spectrum of the Indian earthquake code, IS 1893–1984, are generated by a procedure detailed in the literature [23]. The design spectrum of the Indian earthquake code is derived from the well-accepted design spectrum developed in reference [24]. These time histories are expected to have the characteristics in terms of the energy contents as intended through this well-accepted spectrum, and hence these were used in other studies on seismic behaviour of asymmetric buildings [7, 8, 18]. So, these two uncorrelated artificially generated earthquake time histories having a similar response spectrum are simultaneously used along the two orthogonal axes of the idealized system (i.e., along x- and y-axis in Figure 6).

The responses under near-fault motion are also included in the present study as such responses are found to be crucial for structures in many studies [25–27], particularly if their duration is large. Hence, the responses under idealized fault-parallel and fault-normal motion applied along the x- and y-axis, respectively, of the idealized systems as shown in Figure 6 are also studied. The fault-parallel and fault-normal pulses in simulated idealized form, as used in reference [26], are used in the present study.

4.4. RATE OF STRENGTH AND STIFFNESS DEGRADATION

A large number of experimental load–deformation data for R/C structural members subjected to cyclic loading available in the literature (some of such recent literature, e.g. [9–16], are used here) were studied elsewhere [7, 18]. It is observed from such a study that average drop in strength deterioration δ and average drop in loading stiffness α may be as high as about 10% or even more for inadequate reinforcements and their detailings. However, if reinforcements and their detailings are improved, values of α and δ can be reduced up to 4% and 3% respectively [7, 18]. On the basis of this observation, in the limited scope of the present paper, studies involving the following cases are presented to gauge the effect of the extent of deteriorations: (a) elasto-plastic behaviour, (b) strength deterioration δ is considered to be 10% with the use of the first model, (c) the second model is used with a combination of strength deterioration $\delta = 10\%$ and stiffness degradation $\alpha = 10\%$, (d) the minimum value of strength deterioration parameter $\delta = 3\%$ is used in the first model and (e) in the second model a combination of the minimum stiffness degradation $\alpha = 4\%$ and the minimum strength deterioration $\delta = 3\%$ are used. In the first model, the stiffness degradation parameter is not separately required to be fed in. Cases (b) and (c) attempt to see the effect of the maximum deterioration with two proposed models, while cases (d) and (e) show the effect of the minimum deterioration. The response obtained through the use of all these hysteresis behaviours is compared with the response obtained due to elasto-plastic behaviour to understand their effects clearly.

4.5. METHODOLOGY AND CONVERGENCE

The non-linear equations of motion for the asymmetric systems are derived as follows in terms of the two translational and one rotational degrees of freedom numbered as shown in

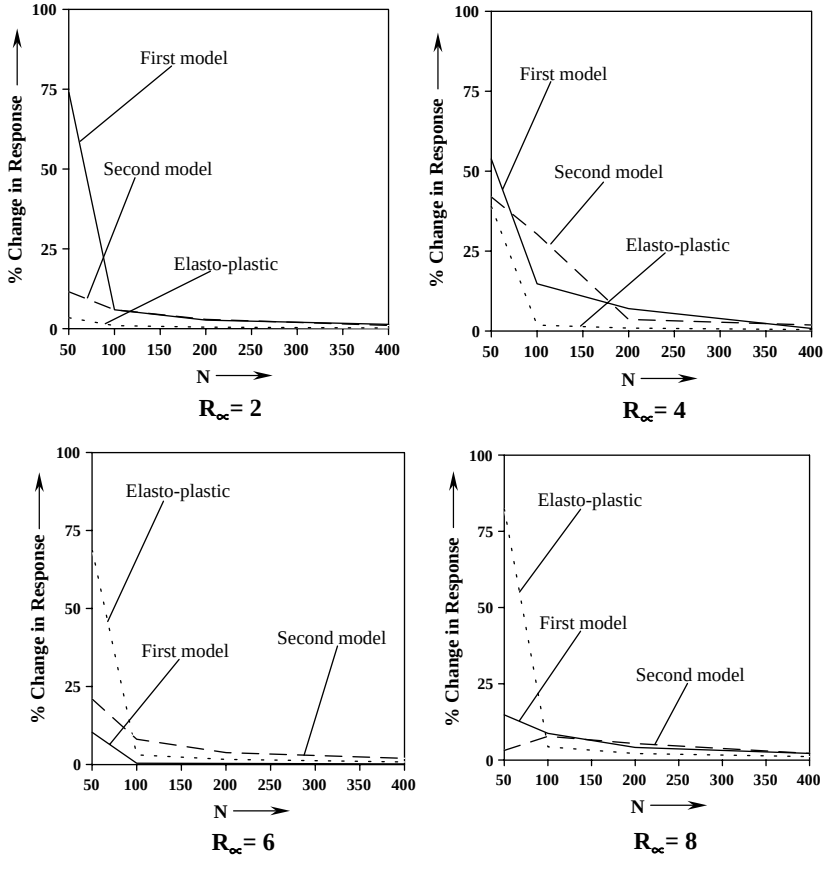

Figure 7. Relative change in displacement response for different values of N for symmetric systems with $T_x = 1{\cdot}0$ s.

Figure 6:

$$\begin{bmatrix} m & 0 & 0 \\ 0 & mr^2 & 0 \\ 0 & 0 & m \end{bmatrix} \begin{Bmatrix} \ddot{u}_x \\ \ddot{\theta} \\ \ddot{u}_y \end{Bmatrix} + [C] \begin{Bmatrix} \dot{u}_x \\ \dot{\theta} \\ \dot{u}_y \end{Bmatrix} + \{f_s\} = - \begin{bmatrix} m & 0 & 0 \\ 0 & mr^2 & 0 \\ 0 & 0 & m \end{bmatrix} \begin{Bmatrix} \ddot{u}_{gx}(t) \\ 0 \\ \ddot{u}_{gy}(t) \end{Bmatrix}, \tag{1}$$

where m is the mass of the rigid deck; r is the radius of gyration of mass of the rigid deck; $[C]$ is the damping matrix; u_x, u_y, θ are the translations of the centre of mass (CM) along the x- and y-axis, and rotation of CM in the horizontal plane respectively; and $\ddot{u}_{gx}$ and $\ddot{u}_{gy}$ are ground accelerations along two mutually perpendicular principal axes respectively.

$\{f_s\}$ is calculated considering the current status of each load-resisting element with the help of hysteresis models. However, in the linear elastic range

$$\{f_s\} = \begin{bmatrix} 4k & 4ke & 0 \\ 4ke & kD^2 & 0 \\ 0 & 0 & 4k \end{bmatrix} \begin{Bmatrix} u_x \\ \theta \\ u_y \end{Bmatrix}. \tag{2}$$

These equations of motion are numerically solved in the time domain by Newmark's β–γ method as in the case of some of the previous studies [e.g., references 21, 28, 29] using the

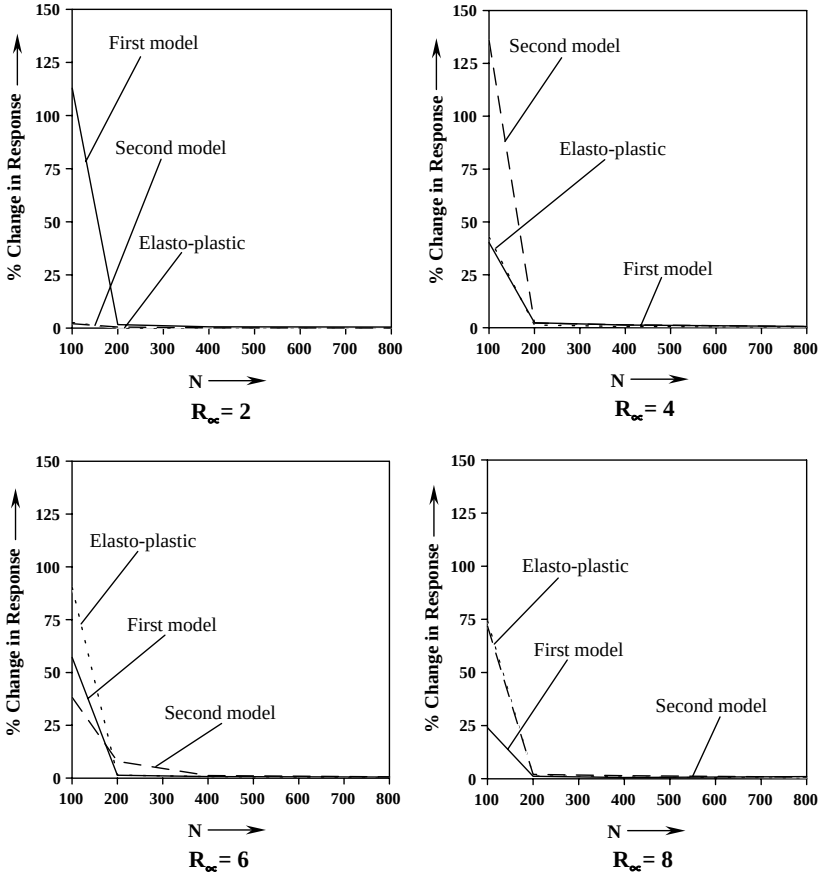

Figure 8. Relative change in displacement response for different values of N for symmetric systems with $T_x = 2{\cdot}0$ s.

modified Newton–Raphson technique. The Newmark's parameters are chosen as $\gamma = 0{\cdot}5$ and $\beta = 0{\cdot}25$.

To ensure accuracy of the numerical process, the results are computed with various sizes of time step given by T_x/N, where T_x is the uncoupled lateral period and N is an integer number which is gradually increased, by doubling it, to obtain the results with better accuracy. With increase in N, the change in displacement response under spectrum-consistent ground motion due to a time step T_x/N relative to the same obtained previously with a time step $T_x/(N/2)$ becomes small for all the models. This percentage change in response is computed as a function of N to study the rate of convergence. Sample results for symmetric systems with $T_x = 1{\cdot}0$ s and $T_x = 2{\cdot}0$ s with four different values of ductility reduction factor, namely $R_\mu = 2, 4, 6, 8$, are presented in Figures 7 and 8 respectively. It is evident from the figures that for all the hysteresis models, with different R_μ values, the change in results is less than about 2·5% only when the time step reduces from $T_x/400$ to $T_x/800$. Hence, a time step of $T_x/400$ may be considered as appropriate for all the further response study using the present models and is also adopted in the rest of the study. It is also interesting to note that the rate at which the accuracy is improved with increase in N due to the proposed hysteresis models is quite comparable or sometimes even better than that exhibited by the elasto-plastic model for higher R_μ values (e.g., $R_\mu = 4$, 6 and 8), i.e., for a larger extent of inelastic behaviour.

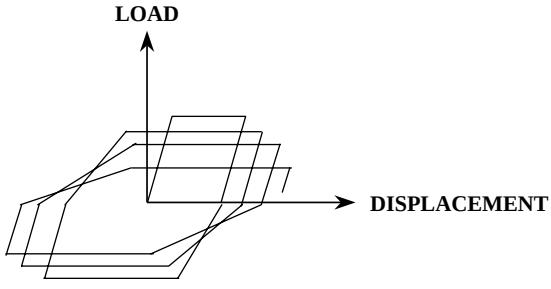

Actual idealised hysteresis behaviour of structural members

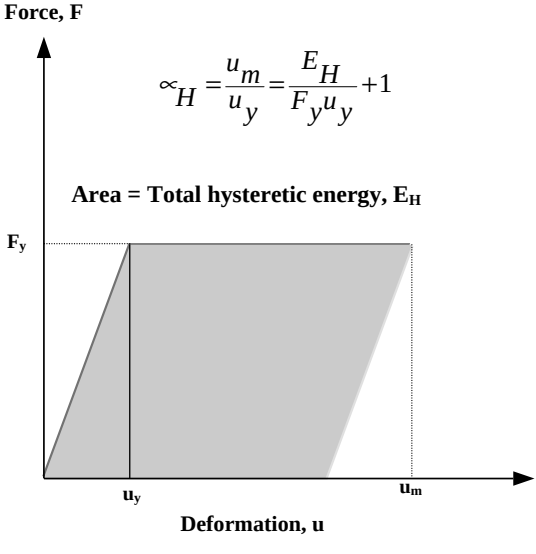

Equivalent elasto-plastic hysteresis behaviour of element under monotonic loading with same amount of hysteretic energy dissipation

Figure 9. Explanation of the concept of normalized hysteretic energy ductility demand after Mahin and Bertero [30].

The damping matrix for the present study is constituted by considering 2% of critical damping in each of the two coupled modes of the asymmetric system in elastic condition.

4.6. RESPONSE STUDY UNDER SPECTRUM-CONSISTENT SYNTHETIC GROUND MOTION

Out of a large number of the response results considering variation of different system parameters, only a few selective results are presented in the limited scope of this paper. An effort has been made to choose the sample cases so that the combination of input parameters can include the extreme values of most of the parameters in some case or other. However, these selective results seem to be sufficient to indicate the notable trends. The maximum displacement and hysteretic energy demand of the flexible and stiff side load-resisting elements of asymmetric six-element systems are normalized with respect to the maximum displacement and hysteretic energy demand, respectively, of a similar reference symmetric system having the same uncoupled lateral period, T_x. Such

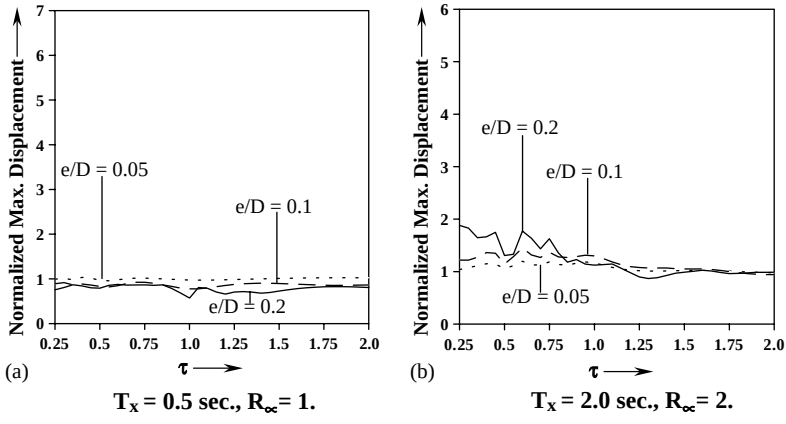

Figure 10. Displacement response of flexible elements of stiffness-eccentric systems with $e_{strength} = e$, using elasto-plastic models.

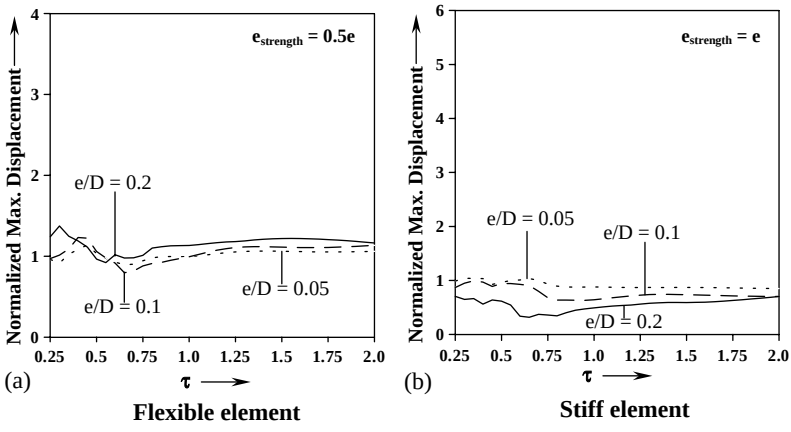

Figure 11. Displacement response of stiffness-eccentric systems with $T_x = 2{\cdot}0$ s, $R_\mu = 4$, using elasto-plastic models.

normalization helps to isolate the effect of asymmetry alone. These normalized response quantities are presented as a function of the uncoupled torsional to lateral period ratio, τ.

The hysteretic energy demand of lateral load-resisting elements was expressed as a factor similar to the displacement ductility demand in previous studies [21, 30]. This factor, which is termed as the normalized hysteretic energy ductility demand (NHEDD), was defined as one plus total hysteretic energy dissipated by the element during all inelastic cycles divided by twice the energy absorbed at the first yield [30]. NHEDD represents the maximum displacement ductility demand in an equivalent elastic–perfectly plastic element that dissipates, under monotonic loading, the same amount of hysteretic energy as the actual element. The concept of this factor is explained through Figure 9 following the literature [30]. Following the same literature [30], NHEDD of any element, μ_H, can be expressed as

$$\mu_H = \frac{u_m}{u_y} = \frac{E_H}{F_y u_y} + 1. \tag{3}$$

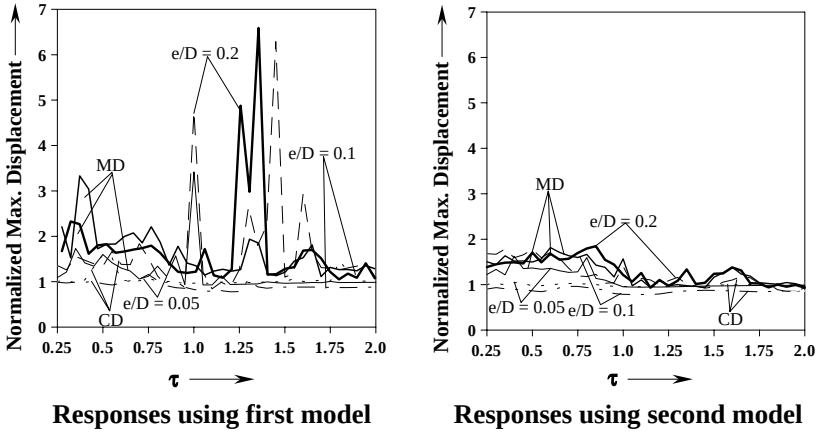

Figure 12. Displacement response of flexible elements of stiffness-eccentric systems with $T_x = 0{\cdot}5$ s, $e_{strength} = e$, $R_\mu = 1$.

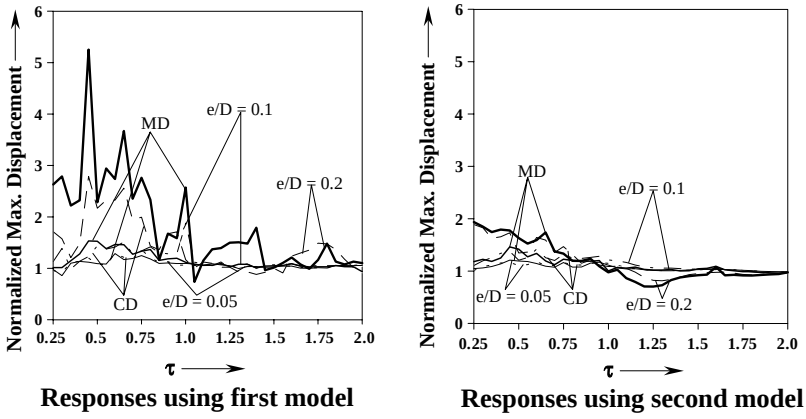

Figure 13. Displacement response of flexible elements of stiffness-eccentric systems with $T_x = 2{\cdot}0$ s, $e_{strength} = e$, $R_\mu = 2$.

The notations used in the above equations can be well understood from Figure 9. The ratio of NHEDD of resisting elements in asymmetric-plan system, μ_H, and that of resisting elements in the corresponding symmetric system, μ_{H0}, is used in the present study to characterize the effect of asymmetry.

Figures 10–15 present sample displacement responses of stiffness-eccentric systems with different lateral periods and ductility-reduction factors. Figures 10 and 11 present responses with elasto-plastic behaviour while Figures 12–15 present the same with proposed hysteresis models. Each of the first two figures present three different curves for the responses of asymmetric systems with small, medium and large eccentricities ($e/D = 0{\cdot}05$, $0{\cdot}1$ and $0{\cdot}2$), respectively. The figures, presenting responses obtained by each of the hysteresis models, have two sets of curves: one corresponding to the maximum value of deterioration parameters and the other to the minimum value. Thus, each of the Figures 12–15 present six curves: three corresponding to the maximum degradation (marked by MD and corresponding to $\delta = 10\%$ for the first model and $\alpha = \delta = 10\%$ for the second one) and drawn with firm lines while the other three corresponding to controlled degradation (marked by CD and corresponding to $\delta = 3\%$ for the first model and $\alpha = 4\%$,

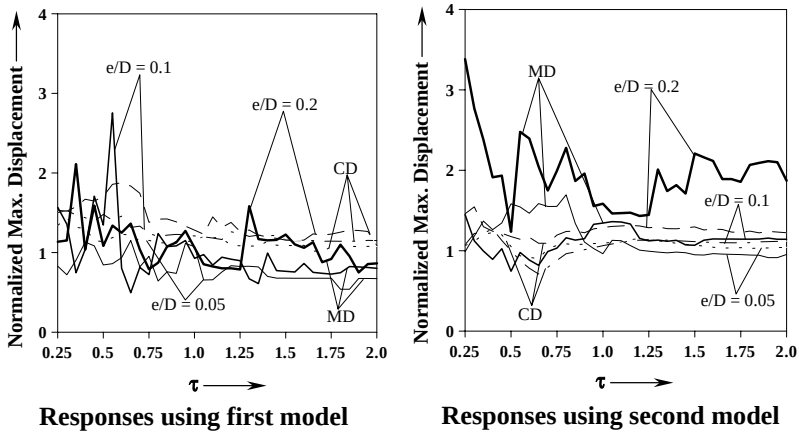

Figure 14. Displacement response of flexible elements of stiffness-eccentric systems with $T_x = 2{\cdot}0$ s, $e_{strength} = 0{\cdot}5e$, $R_\mu = 4$.

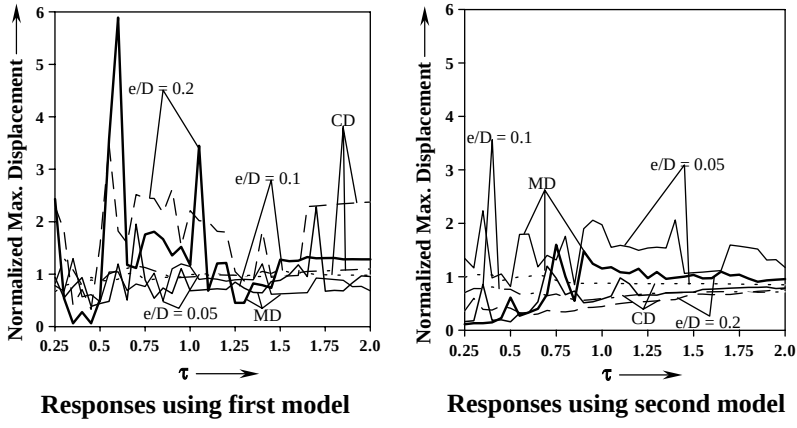

Figure 15. Displacement response of stiff elements of stiffness-eccentric systems with $T_x = 2{\cdot}0$ s, $e_{strength} = e$, $R_\mu = 4$.

$\delta = 3\%$ for the second model) and drawn with dotted lines. Figures 10, 12 and 13 present displacement responses of flexible elements of asymmetric systems having equal strength and stiffness eccentricity ($e_{strength} = e$) with different T_x and R_μ values. On the other hand, Figures 11, 14 and 15 present displacement responses of asymmetric systems with $T_x = 2{\cdot}0$ s and $R_\mu = 4$.

Figures 16–21 present energy responses in terms of normalized NHEDD, μ_H/μ_{H0}, of lateral load-resisting elements of idealized asymmetric systems. Figures 16 and 17 present responses using elasto-plastic behaviour, while responses using proposed hysteresis models are presented in Figures 18–21. Figures 16, 18 and 19 present normalized NHEDD, μ_H/μ_{H0}, of stiffness-eccentric systems having uncoupled lateral period $T_x = 2{\cdot}0$ s, strength eccentricity $e_{strength} = 0{\cdot}5e$ and ductility reduction factor $R_\mu = 2$. Figures 17, 20 and 21 present similar responses of the flexible elements of mass-eccentric systems. Figure 16 contains two sets of curves showing responses of both flexible and stiff elements, respectively, obtained using the elasto-plastic hysteresis model. On the other hand, Figures 18 and 19 present normalized NHEDD, μ_H/μ_{H0} of the flexible and stiff elements respectively. Figures 17(a) and 20 present normalized NHEDD, μ_H/μ_{H0}, of the flexible

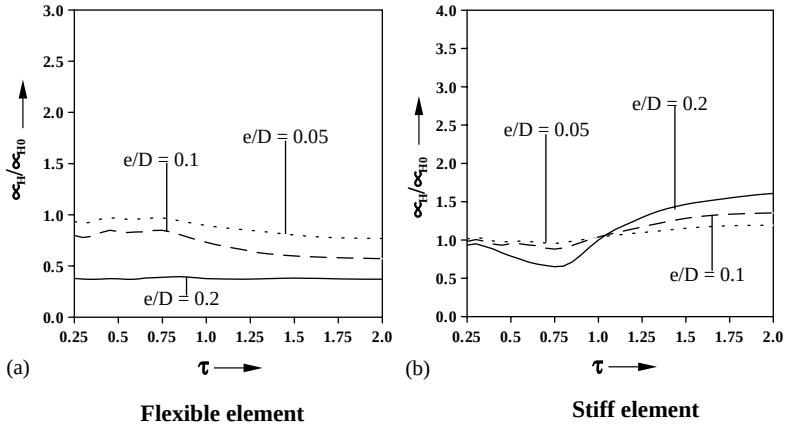

Figure 16. NHEDD of stiffness-eccentric systems using elasto-plastic behaviour with $T_x = 2{\cdot}0$ s, $e_{strength} = 0{\cdot}5e$, $R_\mu = 2$.

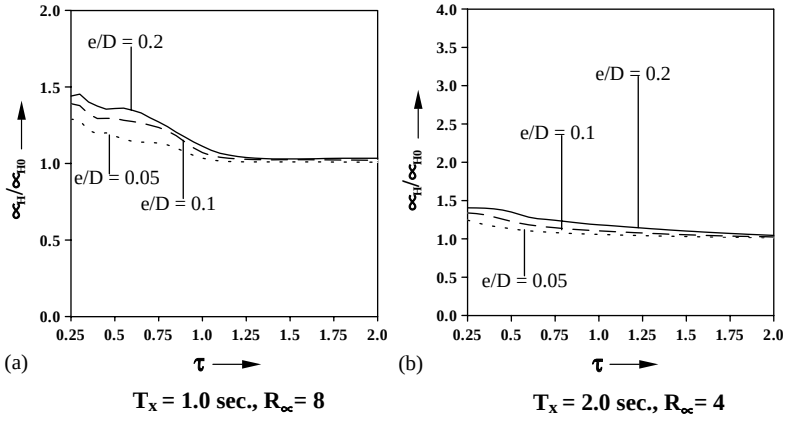

Figure 17. NHEDD of flexible elements of mass-eccentric systems using elasto-plastic behaviour.

elements of mass-eccentric systems with $T_x = 1{\cdot}0$ s and $R_\mu = 8$, while Figures 17(b) and 21 present the same for mass-eccentric systems with $T_x = 2{\cdot}0$ s and $R_\mu = 4$. As in the case of displacement responses, each figure has separate sets of curves obtained using each of the two proposed hysteresis models. Each set again has two different groups of curves: one corresponding to the maximum value of deterioration parameters (marked by MD and corresponding to $\delta = 10\%$ for the first model and $\alpha = \delta = 10\%$ for the second model) and drawn by firm lines and the other corresponding to the minimum value of deterioration parameters (marked by CD and corresponding to $\delta = 3\%$ for the first model and $\alpha = 4\%$, $\delta = 3\%$ for the second model) and drawn by dotted lines. Each group again has three different curves corresponding to the responses of asymmetric systems with small, medium and large eccentricities ($e/D = 0{\cdot}05$, $0{\cdot}1$ and $0{\cdot}2$) respectively.

4.6.1. *Displacement response*

Maximum normalized displacements of flexible elements of stiffness-eccentric systems having $T_x = 0{\cdot}5$ s and $R_\mu = 1$ obtained by using the proposed hysteresis models (Figure 12)

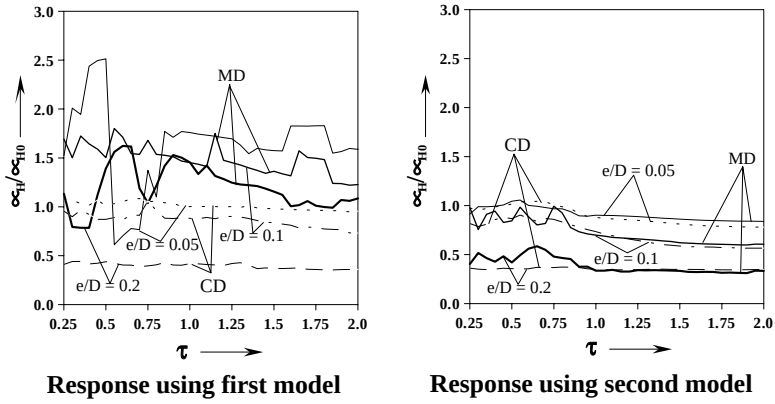

Figure 18. NHEDD of flexible elements of stiffness-eccentric systems with $T_x = 2{\cdot}0$ s, $e_{strength} = 0{\cdot}5e$, $R_\mu = 2$.

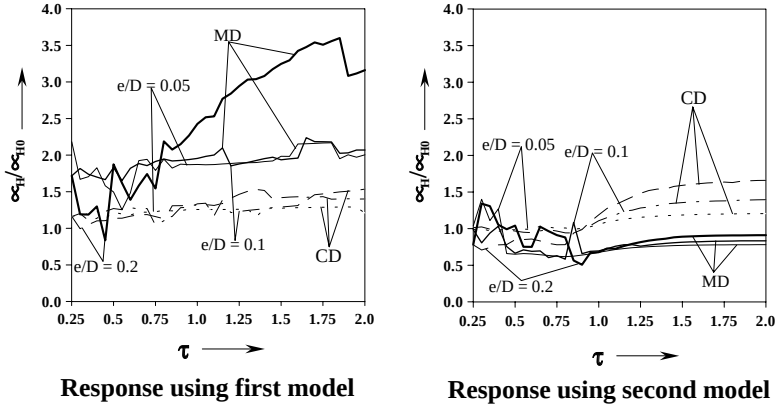

Figure 19. NHEDD of stiff elements of stiffness-eccentric systems with $T_x = 2{\cdot}0$ s, $e_{strength} = 0{\cdot}5e$, $R_\mu = 2$.

are compared with those (Figure 10(a)) obtained by using elasto-plastic models. In a similar fashion, displacement responses of flexible elements of asymmetric systems having $T_x = 2{\cdot}0$ s and $R_\mu = 2$ (Figure 13) using proposed hysteresis models are compared with those obtained by using elasto-plastic models (Figure 10(b)). These comparisons show several times increase in response due to the use of the proposed first model in comparison to the response in corresponding cases due to the elasto-plastic hysteresis models. Similarly, maximum normalized displacement responses of flexible elements (Figure 14) and stiff elements (Figure 15) of stiffness-eccentric systems having $T_x = 2{\cdot}0$ s and $R_\mu = 4$, obtained using proposed hysteresis models, are compared with responses of corresponding systems (Figure 11(a) and 11(b), respectively), obtained by elasto-plastic models. Figures 11(a) and 14 present responses of asymmetric systems with strength eccentricity equal to half the stiffness eccentricity ($e_{strength} = 0{\cdot}5e$), while Figures 11(b) and 15 present the same with equal strength and stiffness eccentricity ($e_{strength} = e$). These comparisons show a considerable increase in response due to the use of the proposed two hysteresis models with maximum values of deterioration parameters in comparison to the response in corresponding cases due to elasto-plastic hysteresis models. This increase may be several times (e.g., even up to about five times) higher than that of the normalized response of elasto-plastic asymmetric

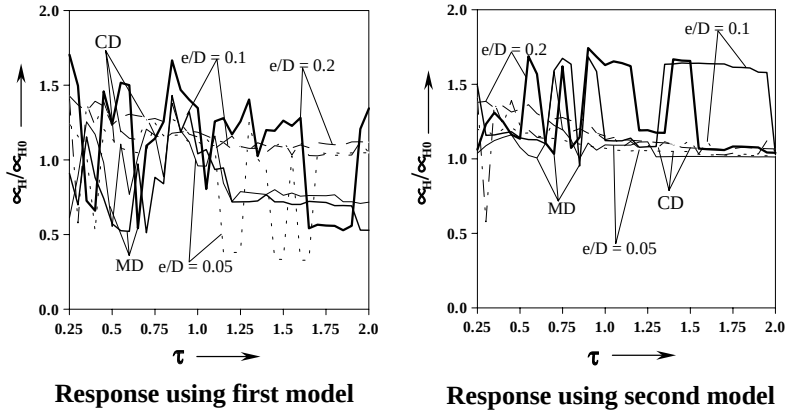

Figure 20. NHEDD of flexible elements of mass-eccentric systems with $T_x = 1{\cdot}0$ s, $R_\mu = 8$.

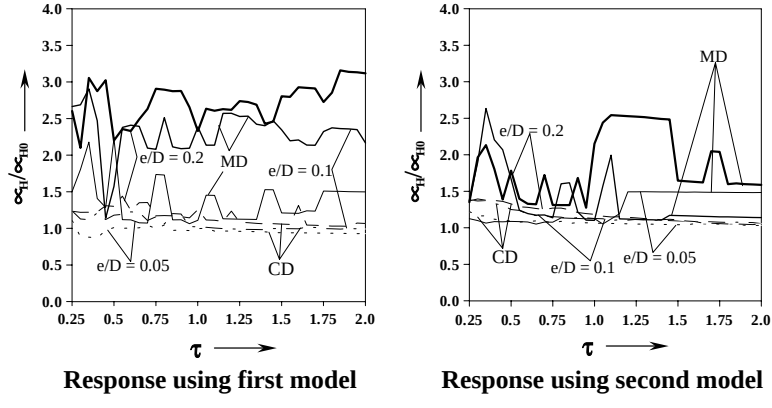

Figure 21. NHEDD of flexible elements of mass-eccentric systems with $T_x = 2{\cdot}0$ s, $R_\mu = 4$.

systems. Figures 13–15 also show that the displacement responses get somewhat reduced when the minimum values of the deterioration parameters are used in the proposed hysteresis models. This implies that the proposed hysteresis models can adequately reflect the extent of progressive torsional damage depending on the rate of deterioration of concrete. The results as a whole show that the deteriorating features of concrete under cyclic loading may cause a many-fold increase in displacement demand in asymmetric concrete structures under seismic excitations. This amplification of displacements could not be recognized in many previous studies due to the use of elasto-plastic models. A comprehensive list of such studies is available in the literature [2].

4.6.2. *Hysteretic energy dissipation capacity demand*

The normalized NHEDD, μ_H/μ_{H0} (presented in Figure 16), of stiff and flexible elements of the stiffness-eccentric systems with $T_x = 2{\cdot}0$ s and $R_\mu = 2$, using elasto-plastic hysteresis models for load-resisting elements, can be compared with the same (presented in Figures 18 and 19) obtained by using proposed hysteresis models. Figures 16(a) and 18 present the variation of μ_H/μ_{H0} for flexible elements, while Figures 16(b) and 19 present the same for stiff elements of the stiffness-eccentric systems. Figures 16(a) and 18 show that μ_H/μ_{H0} of

flexible elements of such long period systems may exhibit an increase of 150% for small eccentricity systems ($e/D = 0{\cdot}05$) to about 300% for large eccentricity systems ($e/D = 0{\cdot}2$), when the maximum value of deterioration parameter ($\delta = 10\%$) is used in the first model, as compared to the same obtained by elasto-plastic hysteresis models. On the contrary, comparison of Figures 16(b) and 19 shows that such an increase is in the order of 133% for large eccentricity systems and about 65% for small eccentricity systems in case of stiff elements of similar systems due to progressively increasing effect of torsion caused by the deterioration of concrete under cyclic loading. Again, due to consideration of the minimum values of stiffness and strength degradation parameters, i.e., $\alpha = 4\%$ and $\delta = 3\%$, the responses corresponding to both of the first and second models are almost the same as those obtained due to the elasto-plastic behaviour of load-resisting elements.

Figures 17(a) and 20 show the variation of normalized NHEDD, μ_H/μ_{H0}, of flexible elements of mass-eccentric systems with lateral period $T_x = 1{\cdot}0$ s, and with ductility reduction factor $R_\mu = 8$, with respect to the variation of τ. Comparison of these two figures shows that for such small period mass-eccentric systems, responses increase marginally even for systems having high-ductility reduction factor for both the hysteresis models when the maximum values of deterioration parameters ($\alpha = \delta = 10\%$) are used. Moreover, for both the models, responses become almost similar to those obtained by using elasto-plastic hysteresis models for lateral load-resisting elements, when the minimum values of deterioration parameters ($\alpha = 4\%$ and $\delta = 3\%$) are used. On the other hand, comparison of Figures 17(b) and 21 shows that for long period ($T_x = 2{\cdot}0$ s) mass-eccentric systems with higher ductility reduction factor ($R_\mu = 4$), normalized NHEDD, μ_H/μ_{H0}, of flexible elements increases considerably (about 80–125%) for both the proposed hysteresis models with maximum values of stiffness- and strength-deterioration parameters, compared to that obtained for the elasto-plastic model. Again, as in the previous case, responses using the proposed two hysteresis models become nearly equal to those obtained by using the elasto-plastic hysteresis model when the minimum values of α and δ are used.

4.6.3. *Discussion on the observed response*

The displacement and energy response, as a whole, show that the first model can pick up the extent of progressive torsional damage quite consistently depending on the values of degrading parameters. The increase in response due to the inclusion of degradation characteristics may be physically explained briefly as follows. Consideration of degradation characteristics in the hysteresis model causes more number of yieldings of the flexible element leading to its consecutive reduction of strength and stiffness compared to that of the stiff elements. Due to the accuracy of the first model, this is, perhaps, more correctly accounted in the response obtained using this model. In this process, the increase in eccentricity caused by the increasing difference of strength and stiffness of flexible and stiff elements causing a shift in the stiffness centre (CS) more towards stiff elements is incorporated rigorously. This increase in eccentricity, in the course of increasing number of yield excursions, implies a shift of CS towards stiff elements, i.e., away from CM. Hence, the effect of asymmetry is increased further. This serious vulnerability of asymmetric buildings made by the R/C frames (due to locally concentrated damage at one edge) as against their counterparts made by steel frames was apprehended in well-accepted literature [2, 3, 21] from the observation of rapid deterioration of R/C members under repetitive loading. However, the effect is found to be more predominant in the displacement response (Figures 12–15), as in this case the maximum displacements which occur perhaps due to the largest pulse are picked up and plotted. In fact, a similar strong effect would have been noticed in NHEDD if it would have been plotted corresponding only to maximum energy dissipated

during the single largest pulse. Since NHEDD considered in the present study is a parameter reflecting cumulative damage during the whole history of shaking, the effect of progressive deterioration appears to be somewhat lesser than that observed in the case of displacement response. The increase in response due to the effect of asymmetry is observed quite less when the elasto-plastic hysteresis model is used, as this model cannot incorporate the gradually increasing effect of progressive torsional damage due to deterioration of R/C structural elements under cyclic loading.

4.7. RESPONSE STUDY UNDER NEAR-FAULT GROUND MOTION

Fault-parallel and fault-normal motions may be considered to have a behaviour like a single pulse. So, the ratio T_x/T_1 of the uncoupled lateral period T_x of the systems to the duration of these pulses, T_1, is found to be the parameter influencing the response instead of the independent value of the uncoupled lateral period T_x of the system [25–27, 29]. The responses of the asymmetric systems corresponding to the three values of T_x/T_1, namely, 0·05, 1·0 and 5·0, are presented. The same ranges of variation of T_x/T_1 were also considered in another study, e.g., reference [29]. The normalized maximum displacement demand for large-eccentricity systems ($e/D = 0{\cdot}2$) with $e_{strength} = 0{\cdot}5e$ and $R_\mu = 1$ under near-fault motion is presented. Near-fault motion involves only a small number of zero crossings and hence a small number of changes in the direction of exerted seismic force. Thus, a system with higher R_μ will perform a very less number of cycles due to its large period resulting from early inelastic range behaviour as well as a less number of direction changes in exerted force due to near-fault motion. However, the systems with $R_\mu = 1$ may undergo at least a few cycles due to their vibrating tendency resulting from primarily governing elastic range behaviour. This may lead to a greater number of yieldings in one of the edge elements than the others. As a result, a larger drop in strength may occur. Hence, the results corresponding to $R_\mu = 1$ are presented for this type of ground motion. Many case studies, corresponding to the combinations arising out of the feasible range of variation of the parameters, are made. Out of such cases, only the results due to the cases described above are presented as these cases can only be expected and found to have strong effect of progressive torsional damage as explained above. Figure 22 presents the maximum displacement response of stiff and flexible elements due to elasto-plastic behaviour. Figure 23 shows the response of flexible elements with two proposed hysteresis models, with two different degrees of degradation for each of the models. Figure 24 presents the response of stiff elements with the same values of the parameters of the proposed models. Comparison of the figures shows that the use of the proposed models can recognize the extent of increase in response depending on the value of the parameter controlling the extent of degradation. Moreover, it is interesting to note that the extent of increase is more in case of the stiff elements of idealized asymmetric systems. This extent of increase may be as high as about 70% more than the corresponding increase of elasto-plastic systems.

5. CONCLUSIONS

The study proposed two simple hysteresis models. The performance of them is judged in predicting a number of experimental curves and the hysteretic energy dissipated by the same. The proposed hysteresis models are also applied for predicting the responses of R/C-asymmetric systems to see whether they can account for progressively increasing torsional response due to strength deterioration and stiffness degradation of R/C

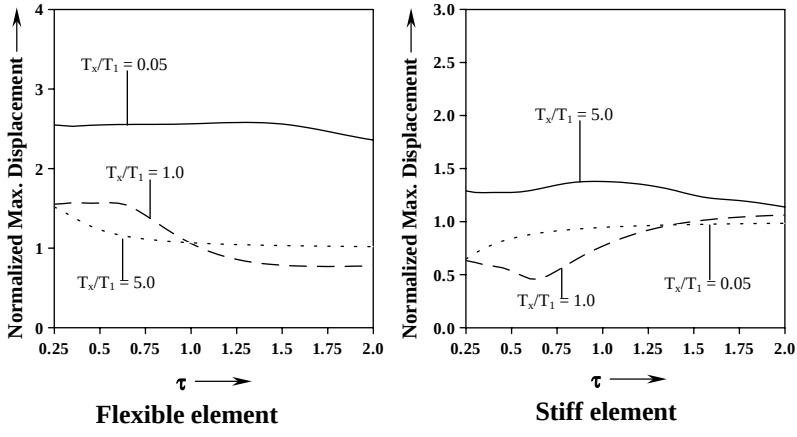

Figure 22. Displacement response of stiffness-eccentric systems using elasto-plastic models under near-fault motion ($R_\mu = 1$, $e_{strength} = 0{\cdot}5e$, $e/D = 0{\cdot}2$).

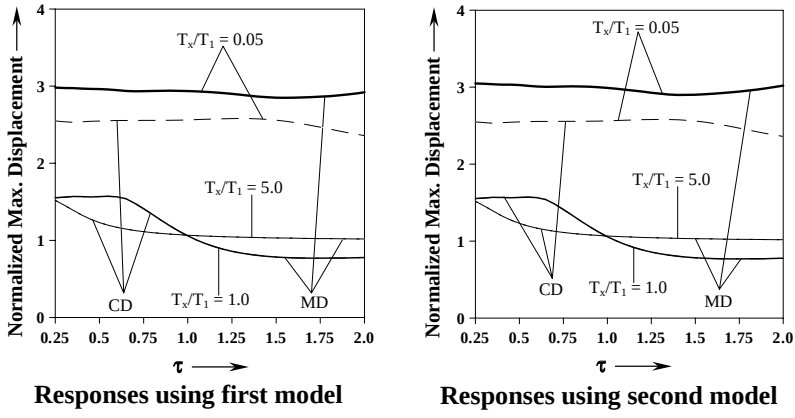

Figure 23. Displacement response of flexible elements of stiffness-eccentric systems under near-fault motion ($R_\mu = 1$, $e_{strength} = 0{\cdot}5e$, $e/D = 0{\cdot}2$).

load-resisting elements. The following broad conclusions can be made from the study:

(1) In comparison with other existing sophisticated models, which require case-specific detailed calibration study, these two models have very few simple and general input parameters, which can be easily calculated. For a general study based on the idealized structural system, these models, especially the first one, can be used very conveniently with the maximum and the minimum value of the parameters for getting upper or lower bound of response. For specific cases, these parameters may be calculated from sample experimental data obtained from cyclic load tests of similar structural elements.
(2) The proposed two simple hysteresis models can predict experimental load–deformation curves of R/C structural members under cyclic loading, with a greater accuracy than the previously used elasto-plastic hysteresis model. Simultaneously accounting for strength-deterioration and stiffness-degradation characteristics of R/C structural elements under cyclic loading, the models, especially the first one, can represent the hysteretic energy dissipation through the inelastic excursions of R/C structural elements

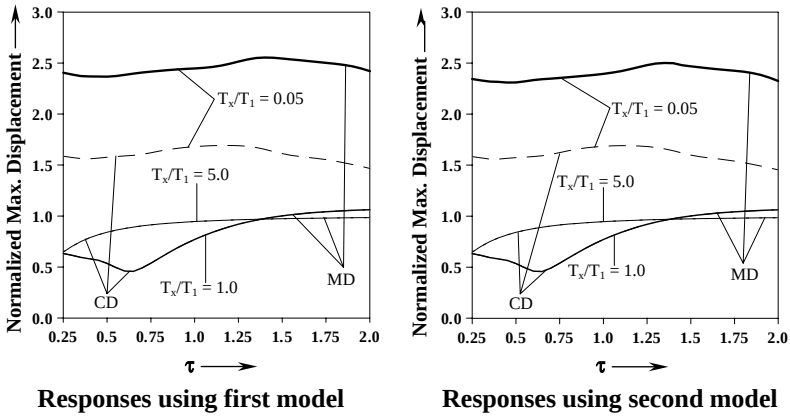

Figure 24. Displacement response of stiff elements of stiffness-eccentric systems under near-fault motion ($R_\mu = 1$, $e_{strength} = 0{\cdot}5e$, $e/D = 0{\cdot}2$).

with considerable accuracy. On the other hand, the hysteretic energy dissipations predicted by elasto-plastic, only stiffness-degrading and only strength-deteriorating models differ considerably from the corresponding experimental values. Among all these models, the first model shows the best performance.

(3) The maximum displacement is a measure of the damage caused by the largest seismic pulse in the applied ground acceleration history while the hysteretic energy demand is a measure of the damage accumulated cumulatively through all the pulses of the ground acceleration history. The proposed two models, particularly the first one, can better recognize the considerable increase in maximum displacement and hysteretic energy dissipation demand due to progressive torsional damage in one edge element than elasto-plastic models.

(4) The same size of the time step, i.e., $T_x/400$, is required to ensure $< 2{\cdot}5\%$ change in results due to a further reduction in time steps, for proposed models as well as elasto-plastic models. This implies that the proposed models require similar computational effort compared to that required for the elasto-plastic model to achieve reasonable accuracy.

(5) In the first model, the changed loading stiffness after yielding is dependent on the amount of plastic deformation in the previous yielding. Hence, this model seems to be more reasonable, and may be used in further studies on seismic torsional behaviour of R/C asymmetric buildings. This model also exhibits superior and accurate performance in all the significant aspects considered in the present study.

The possibility of increased response of edge elements due to strength and stiffness degradation causing progressive torsional damage localized in one side of asymmetric buildings made of R/C frames was hinted at in many previous studies [2, 3, 21, 31]. In fact, the need of detailed research in this direction was pointed out in these studies, but perhaps was not made due to lack of an adequate simplified hysteresis model. In this context, the first model presented in this study seems to be adequate in recognizing the severity of this effect of progressive torsional damage physically hinted at in the literature [2, 3, 21, 31].

ACKNOWLEDGMENTS

The authors sincerely acknowledge the financial help obtained through a project, sanctioned under the *Scheme for Young Scientists* of Department of Science and

Technology, Government of India to the first author, for successful completion of the work presented in the paper.

REFERENCES

1. A. GOYAL, R. SINHA, M. CHAUDHARI and K. JAISWAL 2001 *EERI Preliminary Reconnaissance Report on Earthquake in Gujarat, India, January* 26, 2001. Damage to R/C structures in urban areas of Ahmedabad and Bhuj.
2. A. M. CHANDLER, X. N. DUAN and A. RUTENBERG 1996 *European Earthquake Engineering* **10**, 37–51. Seismic torsional response: assumptions, controversies and research progress.
3. S. C. DUTTA 2001 *Building and Environment* **36**, 1109–1118. Effect of strength deterioration on inelastic seismic torsional behaviour of asymmetric R/C buildings.
4. Y. J. PARK, A. M. REINHORN and S. K. KUNNATH 1987 *National Centre for Earthquake Engineering Research Buffalo, NY, USA*. Report No. NCEER-87-0008 IDARC: inelastic damage analysis of reinforced concrete frame-shear wall structures.
5. Y. S. CHUNG, C. MEYER and M. SHINOZUKA 1990 *ACI Structural Journal* **87**, 326–340. Automated seismic design of reinforced concrete buildings.
6. S. C. DUTTA 1995 *Asian Journal of Structural Engineering* **1**, 36–70. Hysteresis models for nonlinear behaviour of R/C members.
7. P. K. DAS and S. C. DUTTA 2002 *International Journal of Applied Mechanics and Engineering* **7**, 527–564. Effect of strength and stiffness deterioration on seismic behaviour of R/C asymmetric buildings.
8. P. K. DAS and S. C. DUTTA 2001 *Proceedings of National Symposium on Advances in Structural Dynamics and Design*, 9–11 January 2001, Chennai, India, 219–227. Simplified hysteresis models to recognize progressive damage of R.C. asymmetric building under seismic torsion.
9. R. H. BROWN and J. O. JIRSA 1971 *ACI Structural Journal* **68**, 380–390. Reinforced concrete beams under load reversals.
10. M. SAATCIOGLU and G. OZCEBE 1989 *ACI Structural Journal* **86**, 3–12. Response of reinforced concrete columns to simulated seismic loading.
11. P. K. C. WONG, M. J. N. PRIESTLEY and R. PARK 1990 *ACI Structural Journal* **87**, 488–498. Seismic resistance of frames with vertically distributed longitudinal reinforcement in beams.
12. L. E. AYACARDI, J. B. MANDER and A. M. REINHORN 1994 *ACI Structural Journal* **91**, 552–563. Seismic resistance of reinforced concrete frame structure designed only for gravity loads: experimental performance of subassemblages.
13. M. J. N. PRIESTLEY and G. BENZONI 1996 *ACI Structural Journal* **93**, 474–485. Seismic performance of circular columns with low longitudinal reinforcement ratios.
14. C. C. CHEN and G. K. CHEN 1999 *ACI Structural Journal* **96**, 443–449. Cyclic behaviour of reinforced concrete beam–column corner joints connecting spread-ended beams.
15. A. D'AMBRISI and F. C. FILIPPOU 1999 *Journal of Structural Engineering, American Society of Civil Engineers* **125**, 1143–1150. Modeling of cyclic shear behaviour in RC members.
16. Y. L. MO and S. J. WANG 2000 *Journal of Structural Engineering, American Society of Civil Engineers* **126**, 1122–1130. Seismic behaviour of R/C columns with various tie configurations.
17. T. TAKEDA, M. A. SOZEN and N. N. NIELSEN 1970 *Journal of Structural Division, American Society of Civil Engineers* **96**(ST12), 2557–2573. Reinforced concrete response to simulated earthquakes.
18. P. K. DAS and S. C. DUTTA 2000 *Proceedings of ICI-Asian Conference on Ecstasy in Concrete*, 20–22 November, 2000, Bangalore, India, 295–303. Controlling deterioration of RC asymmetric buildings under seismic loadings.
19. J. C. CORRENZA, G. L. HUTCHINSON and A. M. CHANDLER 1992 *Soil Dynamics and Earthquake Engineering* **11**, 465–484. A review of reference models for assessing inelastic seismic torsional effects in buildings.
20. C. M. WONG and W. K. TSO 1995 *Journal of Structural Engineering, American Society of Civil Engineers* **121**, 1436–1442. Evaluation of seismic torsional provisions in uniform building code.
21. R. K. GOEL 1997 *Journal of Structural Engineering, American Society of Civil Engineers* **123**, 1444–1453. Seismic response of asymmetric systems: energy-based approach.
22. NEHRP 1991 *Report No. FEMA* 222, *Federal Emergency Management Agency, Washington, DC, USA, January*. NHERP recommended provisions for the development of seismic regulations for new buildings (1992), Part I: provisions.

23. M. R. KHAN 1987 *Earthquake Engineering and Structural Dynamics* **15**, 985–992. Improved method of generation of artificial time-histories, rich in all frequencies.
24. G. W. HOUSNER 1959 *Proceedings of American Society of Civil Engineers, Engineering Mechanics Division* **85**, 109–129. Behaviour of structures during earthquakes.
25. R. K. GOEL and A. K. CHOPRA 1990 *Earthquake Engineering and Structural Dynamics* **19**, 949–970. Inelastic seismic response of one-storey, asymmetric-plan systems: effects of stiffness and strength distribution.
26. C. V. R. MURTY and J. F. HALL 1994 *Earthquake Engineering and Structural Dynamics* **23**, 1199–1218. Earthquake collapse analysis of steel frames.
27. F. NAEIM 1995 *Earthquake Spectra* **11**, 91–109. On seismic design implications of the 1994 Northridge earthquake records.
28. A. K. CHOPRA and R. K. GOEL 1991 *Journal of Structural Engineering, American Society of Civil Engineers* **117**, 3762–3782. Evaluation of torsional provisions in seismic codes.
29. R. K. GOEL and A. K. CHOPRA 1994 *Journal of Structural Engineering, American Society of Civil Engineers* **120**, 161–179. Dual-level approach for seismic design of asymmetric-plan buildings.
30. S. A. MAHIN and V. V. BERTERO 1981 *Journal of Structural Engineering, American Society of Civil Engineers* **107**, 1777–1795. An evaluation of inelastic seismic design spectra.
31. S. C. DUTTA, S. K. JAIN and C. V. R. MURTY 2001 *Journal of Sound and Vibration* **242**, 151–167. Inelastic seismic torsional behaviour of elevated tanks.